
EXACT: How to Train Your Accuracy

Ivan Karpukhin¹ Stanislav Dereka¹ Sergey Kolesnikov¹

Abstract

Classification tasks are usually evaluated in terms of accuracy. However, accuracy is discontinuous and cannot be directly optimized using gradient ascent. Popular methods minimize cross-entropy, Hinge loss, or other surrogate losses, which can lead to suboptimal results.

In this paper, we propose a new optimization framework by introducing stochasticity to a model's output and optimizing expected accuracy, i.e. accuracy of the stochastic model. Extensive experiments on image classification show that the proposed optimization method is a powerful alternative to widely used classification losses.

1. Introduction

Accuracy is one of the most used evaluation metrics in computer vision (LeCun et al., 1998; Krizhevsky et al., 2009; 2012), natural language processing (Maas et al., 2011; Zhang et al., 2015), and tabular data classification (Arik & Pfister, 2021). While accuracy naturally appears in classification tasks, it is discontinuous and difficult to optimize directly. For classification, multiple surrogate losses were proposed, including cross-entropy and Hinge loss (Wang et al., 2022). Previous works show that these training objectives correlate with accuracy, but there is no direct connection. In our toy example we demonstrate that decreasing cross-entropy or Hinge loss can lead to a drop in accuracy, and vice versa.

In this work, we take a different approach to accuracy optimization in the context of deep learning. Our idea is to make accuracy differentiable by introducing stochasticity into a model's output. For the stochastic model, we evaluate expected accuracy, which is differentiable and can be maximized via gradient ascent. We call the proposed method EXpected ACcuracy opTimization (EXACT). It optimizes accuracy under the assumption of stochastic prediction and thus can be considered a direct optimization technique in

¹Tinkoff. Correspondence to: Ivan Karpukhin <i.a.karpukhin@tinkoff.ru>.

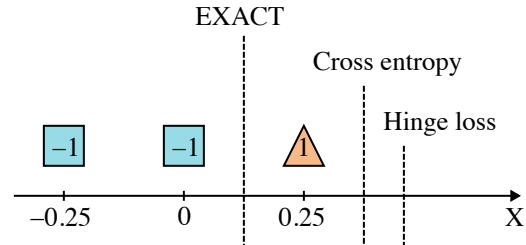


Figure 1. Decision boundaries found by cross-entropy loss, Hinge loss and the proposed EXACT method. EXACT achieves 100% accuracy, while cross-entropy and Hinge loss misclassify one element.

contrast to surrogate losses.

Contributions of this work can be summarized as follows:

1. We propose a new optimization framework for classification tasks.
2. We provide an efficient method for evaluating the proposed loss function and its gradient².
3. We compare the quality of the proposed method with cross-entropy and Hinge losses on popular image classification datasets. According to our results, in most cases, the proposed approach produces results on par with or better than other methods.

2. Related Work

2.1. Classification Losses

One of the most used classification loss functions is cross-entropy (CE), also known as negative log-likelihood (Wang et al., 2022). Minimization of CE reduces the difference between predicted posterior class probabilities and true posteriors. Cross-entropy is largely motivated by the Bayes optimality theorem (Rosasco et al., 2004): if a model estimates true posterior probabilities, then it achieves maximum

²<https://github.com/tinkoff-ai/exact>

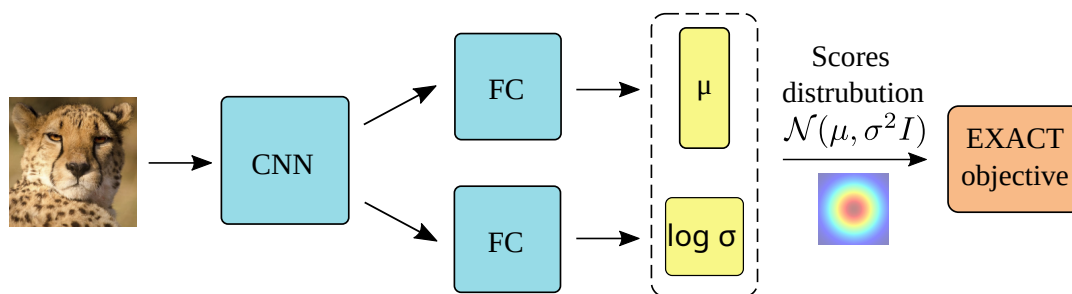


Figure 2. EXACT image classification training pipeline. CNN model is followed by fully-connected (FC) mean and variance prediction subnetworks. EXACT’s training objective is applied to the distribution of class scores vector.

accuracy. However, Bayes optimality is rarely achieved in practice due to limitations of model architectures and optimization techniques. On the other hand, there are usually many different models with a maximum accuracy property, and the Bayes classifier is only one of them.

Another loss function, widely used for classification tasks, is Hinge loss (Gentile & Warmuth, 1998). It is motivated by a support-vector machine (SVM) (Rosasco et al., 2004). Unlike CE, Hinge loss stops training when scores of ground truth classes exceed alternative scores with the required margin. In some problems, Hinge loss shows results on par or better than cross-entropy (Epalle et al., 2021; Jin et al., 2014; Ozyildirim & Kiran, 2021; Peng & Liu, 2018).

Loss functions, such as cross-entropy and Hinge loss, correlate with accuracy, but do not optimize it directly. For this reason, these methods are referred to as proxy or surrogate losses (Grabocka et al., 2019). In this work, we propose a different approach and directly optimize the accuracy of a specially designed stochastic model.

2.2. Surrogate Losses

Most deep learning methods rely on gradient descent optimization, which is applicable only to differentiable loss functions. Surrogate losses provide differentiable approximations for non-differentiable target metrics. The concept of surrogate losses goes beyond accuracy optimization. In binary classification, there are well-known approximations for the AUC ROC metric (Calders & Jaroszewicz, 2007). For example, AUC ROC can be rewritten in terms of the Heaviside step function, which is approximated via a logistic function or polynomials. Direct AUC ROC optimization techniques involve repeated AUC ROC computation over the dataset, which is usually computationally expensive.

Special loss functions were proposed in domains such as metric learning and ranking (Kaya & Bilge, 2019; Calauzenes et al., 2012). Many of them use margin-based

losses, similar to Hinge loss (Weinberger & Saul, 2009). Some surrogate losses formulate target metrics in terms of the Heaviside step function, which is then approximated by smooth functions (Patel et al., 2021).

The proposed EXACT method is designed for accuracy optimization. However, the idea of using stochastic predictions can potentially be applied in other machine learning domains.

2.3. Probabilistic Embeddings

There are multiple ways to introduce stochasticity to the model output. One way is to use probabilistic embeddings (PE) (Shi & Jain, 2019; Karpukhin et al., 2022), where the model predicts a distribution of outputs rather than a single vector. For example, the model can predict a mean and covariance matrix of the multivariate normal distribution. This concept was used in many deep learning approaches, such as regression via mixture density networks (Bishop, 1994), variational auto-encoders (Kingma & Welling, 2014), and metric learning (Chang et al., 2020).

One part of the proposed EXACT method is probabilistic prediction, which is similar to PE. However, unlike previous approaches, we use stochastic prediction for expected accuracy optimization.

2.4. Bayesian Neural Networks

Bayesian neural networks (BNNs) (Goan & Fookes, 2020) are another method used to introduce stochasticity to a model. In BNNs, the model weights are treated as random variables, and the output depends on particular weights’ values. Expected accuracy optimization, proposed in our work, can potentially be applied to the output of the BNN. However, we decided to use probabilistic embeddings, where uncertainty is the function of input data.

3. Motivation

Let us consider a toy example where cross-entropy and Hinge losses produce suboptimal results in terms of accuracy. Suppose we solve a binary classification problem via the simple threshold model $f(x) = x - b$. The model predicts class y based on the sign of $f(x)$:

$$y = \begin{cases} -1, & f(x) < 0 \\ 1, & f(x) \geq 0 \end{cases} \quad (1)$$

The goal of training is to fit a threshold parameter b . Suppose the training set consists of three points: -0.25, 0, and 0.25. The first two points have the label $l = -1$, and the last point has the label 1, as shown in Figure 1.

Cross-entropy loss for binary classification is usually applied to the output of the logistic function g , which converts $f(x)$ to the probability of the positive class:

$$\mathcal{L}_{CE}(x, l) = -\log g(lf(x)), \quad (2)$$

$$g(x) = \frac{1}{1 + e^{-x}}. \quad (3)$$

Binary Hinge loss is computed as follows:

$$\mathcal{L}_{Hinge}(x, l) = \max(0, 1 - lf(x)). \quad (4)$$

We performed optimization via grid search and found, that minimizing cross-entropy and Hinge losses fails to find the optimal value of b , which must be in the interval $(0, 0.25)$. Cross-entropy loss leads to $b = 0.7$, and Hinge loss produces $b = 0.75$. Gradient ascent optimization of the proposed EXACT method, which we describe below, achieves perfect classification in this example, leading to $b = 0.125$.

4. EXACT

The accuracy metric is not differentiable and cannot be directly optimized via gradient ascent. The core idea behind EXACT is to introduce stochasticity to the model output and then optimize the expected accuracy, i.e. accuracy of the stochastic model.

4.1. Definitions

The goal of classification training is to minimize the empirical risk of mapping $x \rightarrow y$, where $x \in \mathcal{R}^d$ is an input feature vector and $y \in \overline{1, C}$ is a class label. In deep learning, the problem is usually solved by a parametric differentiable function $f_\theta : \mathcal{R}^d \rightarrow \mathcal{R}^C$, which predicts score vectors (or logits) of output classes. Prediction is obtained by taking the class with the maximum score:

$$\tilde{y}_\theta(x) = \arg \max_{i \in \overline{1, C}} (f_\theta(x))_i. \quad (5)$$

In this work, we consider accuracy maximization, i.e. maximization of the correct classification probability of elements (x, y) from some dataset:

$$\mathcal{A}(\theta) = \mathbb{E}_{x, y} \mathbb{I}(\tilde{y}_\theta(x) = y). \quad (6)$$

$$\hat{\theta} = \arg \max_{\theta} \mathcal{A}(\theta), \quad (7)$$

where $\hat{\theta}$ is an optimal set of parameters that we try to approximate using gradient ascent.

4.2. Expected Accuracy

Let us consider a modification of the function $f : x \rightarrow (\mu, \sigma)$, which predicts the multivariate normal distribution of a score vector rather than a single vector:

$$s \sim \mathcal{N}(\mu(x), \sigma^2(x)I), \quad (8)$$

$$\tilde{y}_\theta(s) = \arg \max_{i \in \overline{1, C}} s_i. \quad (9)$$

In this case, the predicted class $\tilde{y}_\theta(s)$ is a discrete random variable, which depends on the value of the score vector s . Accuracy becomes a random variable, and we can estimate the expected accuracy:

$$\mathbb{E}\mathcal{A}(\theta) = \mathbb{E}_{x, y} \mathbb{E}_s \mathbb{I}(\tilde{y}_\theta(s) = y) \quad (10)$$

$$= \mathbb{E}_{x, y} \mathbb{P}(\tilde{y}_\theta(s) = y) \quad (11)$$

$$= \mathbb{E}_{x, y} \mathbb{P}(s_y > \max_{i \neq y} s_i), \quad (12)$$

where \mathbb{I} is an indicator function. As we will show below, expected accuracy is differentiable w.r.t. mean vector μ . This property makes optimization via gradient ascent possible.

4.3. Optimization

In this section, we propose an effective approach to expected accuracy computation and differentiation. We base this method on reducing the original problem to an orthant integration of the multivariate normal probability density function (PDF). The latter can be effectively computed using algorithms proposed in previous works.

Definition 4.1. Delta matrix D_y of the order C for the ground truth label y is a matrix of size $C - 1 \times C$ with

$$D_{y_{i,j}} = \begin{cases} 1, & j = y \\ -1, & j < y, i = j \\ -1, & j > y, i = j - 1 \\ 0, & \text{otherwise} \end{cases}. \quad (13)$$

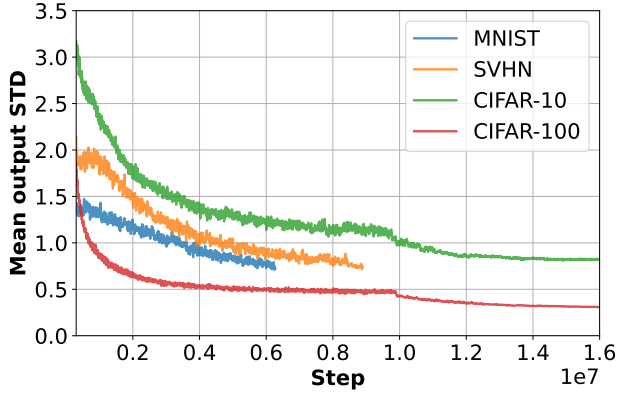


Figure 3. Predicted uncertainty (multivariate normal STD) training dynamics. Average uncertainty reduces during training, narrowing the gap between accuracy and expected accuracy.

In other words, the delta matrix has the following form:

$$D_y = \begin{bmatrix} -1 & 0 & \dots & 0 & 1 & 0 & \dots & 0 \\ 0 & -1 & \dots & 0 & 1 & 0 & \dots & 0 \\ & & \ddots & & \vdots & & \ddots & \\ 0 & 0 & \dots & -1 & 1 & 0 & \dots & 0 \\ 0 & 0 & \dots & 0 & 1 & -1 & \dots & 0 \\ & & \ddots & & \vdots & & \ddots & \\ 0 & 0 & \dots & 0 & 1 & 0 & \dots & -1 \end{bmatrix}. \quad (14)$$

Now we can state a core result, necessary for expected accuracy evaluation.

Theorem 4.2. *Suppose the score vector s is distributed according to multivariate normal distribution $\mathcal{N}(\mu, \sigma^2 I)$ in \mathbb{R}^C . In this case, the probability of the y -th score exceeding other scores can be computed as*

$$P(s_y > \max_{i \neq y} s_i) = \int_{\Omega_+} \mathcal{N}(t; \frac{D_y \mu}{\sigma}, D_y D_y^T) dt, \quad (15)$$

where D_y is a delta matrix of the order C for label y and $\Omega_+ : \{t \in \mathbb{R}^{C-1}, t_i \geq 0, i = \overline{1, C-1}\}$ is an orthant in \mathbb{R}^{C-1} .

The orthant integral in equation 15 can be effectively computed using the Genz algorithm (Genz, 1992). The equation contains the expected accuracy for a single element of the dataset. Total expected accuracy is computed according to equation 12 as an average of expected accuracies for all elements.

Gradient ascent requires gradient computation w.r.t. parameters μ and σ . Both parameters are contained only in the

mean part of the normal distribution in equation 15. Suppose

$$m = \frac{D_y \mu}{\sigma}, \quad (16)$$

$$\Sigma = D_y D_y^T. \quad (17)$$

Now we can estimate the gradients of the expected accuracy w.r.t. mean vector m .

Theorem 4.3. *Suppose the vector s is distributed according to multivariate normal distribution $\mathcal{N}(m, \Sigma)$ in \mathbb{R}^{C-1} and \hat{s}_i is a random vector of all elements in s except i -th, conditioned on $s_i = -m_i$. Then \hat{s}_i is normally-distributed with some parameters \hat{m}_i and $\hat{\Sigma}_i$ and*

$$\left(\int_{\Omega_+} \mathcal{N}(t; m, \Sigma) dt \right)_{m_i} = \mathcal{N}(0; m_i, \Sigma_{i,i}) \int_{\Omega'_+} \mathcal{N}(t; \hat{m}_i, \hat{\Sigma}_i) dt, \quad (18)$$

where $\Omega'_+ : \{t \in \mathbb{R}^{C-2}, t_i \geq 0, i = \overline{1, C-2}\}$ is an orthant in \mathbb{R}^{C-2} .

Same as before, the orthant integral can be computed using the Genz algorithm (Genz, 1992). According to Theorem 4.3 and Equation 16, expected accuracy is differentiable w.r.t. both $\mu(x)$ and $\sigma(x)$. The gradient descent method can be applied to minimize the negative value of the expected accuracy. When expected accuracy is close to zero, the gradient norm can be small. To speed up training at the beginning, we optimize the negative logarithm of the expected accuracy rather than its absolute value.

4.4. The Role of Uncertainty

The EXACT model predicts class scores μ and uncertainty σ . Here, we provide some intuition about the role of uncertainty in the training process. When uncertainty is close to zero, stochastic output reduces to the point prediction, similar to a traditional neural classifier. In the latter case, there is no difference between accuracy and expected accuracy. At the same time, small uncertainty leads to a small gradient norm and prevents training.

EXACT is able to automatically adjust uncertainty levels to achieve stable training. When the probability of the correct classification in Equation 12 is large, EXACT tends to reduce uncertainty. On the other hand, when the probability of the correct classification is small, uncertainty grows. This leads to the natural balance between small and large uncertainty values. Empirical results show that average uncertainty reduces during training. Corresponding training curves are presented in Figure 3.

Table 1. Comparison of EXACT with cross-entropy loss (CE) for different CNN architectures using the SGD optimizer.

Dataset	ResNet		Wide ResNet		EfficientNet		PyramidNet	
	EXACT	CE	EXACT	CE	EXACT	CE	EXACT	CE
MNIST	99.63	99.70	99.65	99.67	99.63	99.70	99.66	99.67
SVHN	97.09	96.80	97.30	96.91	97.23	97.14	97.88	97.82
CIFAR-10	95.28	95.09	95.76	95.45	94.68	94.61	97.14	96.96
CIFAR-100	77.92	76.31	79.50	78.09	75.39	76.59	85.60	85.97

Table 2. Comparison of EXACT with cross-entropy loss (CE) and Hinge losses for Wide ResNet architecture and different optimizers.

Dataset	EXACT	SGD		EXACT	Adam		EXACT	ASAM	
		HINGE	CE		HINGE	CE		HINGE	CE
MNIST	99.66	99.69	99.67	99.54	99.36	99.51	99.73	99.75	99.73
SVHN	97.30	96.85	96.91	95.80	95.32	95.52	97.76	97.67	97.80
CIFAR-10	95.76	95.50	95.45	88.86	84.53	88.65	96.40	95.62	96.10
CIFAR-100	79.50	77.51	78.09	64.53	46.06	61.98	80.96	78.51	80.81

4.5. Inference

During inference, EXACT predicts score vectors with maximum density, i.e. μ vector. The uncertainty prediction head can be excluded from the model in inference time, leading to zero computational overhead. An alternative way to make predictions is to sample from the output distribution. Based on a small set of experiments, sampling does not give accuracy improvements, but rather introduces noise into predictions.

5. Experiments

In this work, we aim to answer the following questions: (1) how does EXACT performance correspond to that of cross-entropy and Hinge losses, (2) how to choose EXACT hyperparameters, and (3) how big is the computational overhead of the proposed EXACT method? To answer these questions, we analyze EXACT in the context of deep image classification by using the MNIST (LeCun et al., 1998), SVHN (Netzer et al., 2011), CIFAR-10, and CIFAR-100 (Krizhevsky et al., 2009) datasets. Below, we describe training details and experimental results.

5.1. Training Details

We compare 4 model architectures: ResNet-18 (He et al., 2016), Wide ResNet-16-8 (Zagoruyko & Komodakis, 2016), EfficientNet-v2-M (Tan & Le, 2019) and PyramidNet-272 (Han et al., 2017). In ResNet and EfficientNet, we scale images to size 256. For Wide ResNet and PyramidNet, we set image size to 32 to make a pooling size the same in our models. In all experiments, we apply the Autoaugment (Cubuk et al., 2019) augmentation tuned for CIFAR10. We also apply random horizontal flipping during training for

images from CIFAR10 and CIFAR100.

We consider three optimizers: stochastic gradient descent with momentum (SGD) (Sutskever et al., 2013), Adam (Kingma & Ba, 2014), and the recently proposed Asam optimizer (Kwon et al., 2021). All models are trained for 90 epochs on MNIST and SVHN, and for 500 epochs on CIFAR10 and CIFAR100. We use a reduce-on-plateau learning rate scheduler with an initial learning rate equal to 0.5 and a drop factor of 0.3. We use the PyTorch deep learning framework (Paszke et al., 2019). Each experiment is performed using a single Nvidia V100 GPU.

5.2. Classification Quality

We compared EXACT with surrogate losses in multiple setups. First, we evaluated different neural network architectures, trained with cross-entropy and EXACT losses. Results are presented in Table 1. All models were trained using stochastic gradient descent (SGD) with the momentum equal to 0.9. In 10 out of 16 cases, EXACT achieved higher accuracy than cross-entropy.

We also compared training with different optimizers for cross-entropy, Hinge loss, and EXACT. For this purpose, we chose Wide ResNet, as it achieves better results than ResNet and EfficientNet while being 12 times faster than PyramidNet. Results are presented in Table 2. EXACT achieved higher accuracy in 9 out of 12 comparisons.

5.3. Sample Size

EXACT depends on the sample size used in the Genz integration algorithm (Genz, 1992). We performed experiments with different sample sizes using the Wide ResNet architecture and ASAM optimizer. According to the experiments

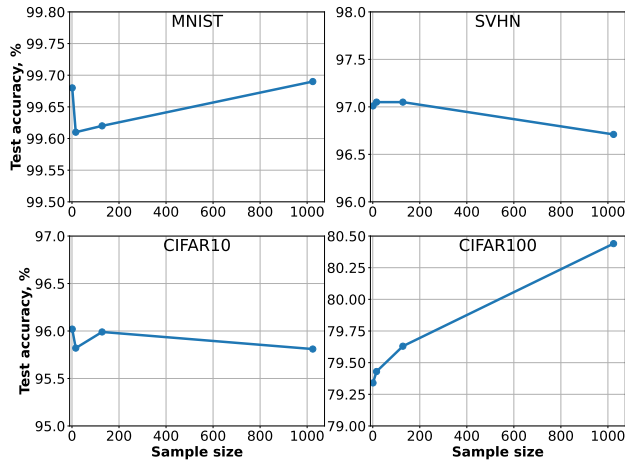


Figure 4. EXACT test accuracy dependency on the sample size on different datasets. Results are presented for Wide ResNet and ASAM optimizer.

above, this setup leads to high test-time accuracy while being 12 times more computationally efficient than PyramidNet. Results are presented in Figure 4. On MNIST, SVHN, and CIFAR-10, the sample size has minor effects on accuracy. Even training with sample size 1 produces results on par with larger samples. On CIFAR-100, a larger sample size leads to higher accuracy.

5.4. Computational Complexity

EXACT memory consumption and computational efficiency depend on the number of classes C and sample size N . The most expensive part of the algorithm is gradient computation, which requires $O(NC^2)$ in terms of both operations and memory. Empirical memory usage per data element and computational efficiency (milliseconds per data element) are presented in Figure 5. Evaluations for different numbers of classes were made with a sample size equal to 512. Different sample sizes were evaluated with the number of classes equal to 128. Performance was evaluated for batches of size 256.

Relative EXACT overhead largely depends on the number of classes and model architecture. For example, EXACT with the sample size equal to 512 in the case of 16 classes reduces training RPS by 8% for ResNet-34. For larger models, relative loss overhead is smaller and vice versa.

6. Discussion

While previous works on deep classification minimized surrogate losses, EXACT directly optimizes the accuracy of the model with stochastic prediction. The benefits of accuracy optimization were illustrated in our toy example, where both

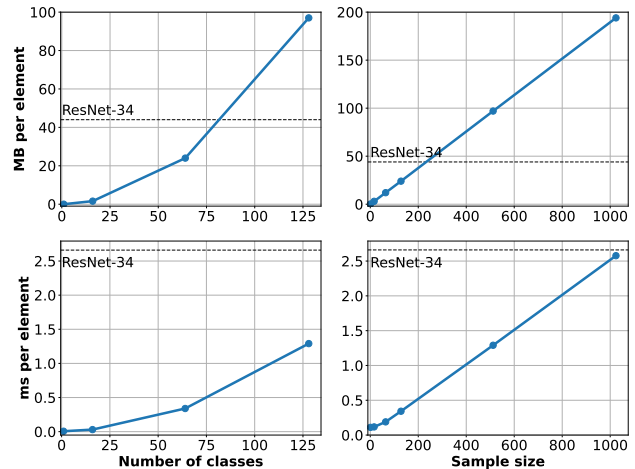


Figure 5. EXACT loss memory consumption (MB per element) and computation speed (ms per element) for different numbers of classes and sample sizes. Performance is compared to the ResNet-34 neural network.

cross-entropy and Hinge losses failed to solve the problem. The proposed EXACT method treats non-differentiable quality metrics in a novel way which can potentially be applied to domains beyond classification, such as metric learning, ranking, etc.

According to our experiments, EXACT leads to competitive results on a number of image classification tasks. In many cases, EXACT achieves higher classification accuracy with a computational overhead of about 10%. While computational efficiency is dependent on sample size, we show that EXACT can be trained even with single-point estimation. Extra computational resources can be used to further increase EXACT accuracy.

7. Conclusion

We presented EXACT, a novel approach for optimizing stochastic model accuracy via gradient ascent. Our results show that EXACT achieves higher accuracy than cross-entropy and Hinge losses in several image classification tasks (SVHN, CIFAR10, and CIFAR100). EXACT can be effectively implemented in popular deep learning frameworks, including PyTorch, leading to the computational overhead of about 10% depending on the number of classes and neural model complexity.

References

- Arık, S. O. and Pfister, T. Tabnet: Attentive interpretable tabular learning. In *AAAI*, volume 35, pp. 6679–6687, 2021.

- Bishop, C. M. Mixture density networks. 1994.
- Calauzenes, C., Usunier, N., and Gallinari, P. On the (non-) existence of convex, calibrated surrogate losses for ranking. *Advances in Neural Information Processing Systems*, 25, 2012.
- Calders, T. and Jaroszewicz, S. Efficient auc optimization for classification. In *European conference on principles of data mining and knowledge discovery*, pp. 42–53. Springer, 2007.
- Chang, J., Lan, Z., Cheng, C., and Wei, Y. Data uncertainty learning in face recognition. In *Proceedings of the IEEE/CVF Conference on Computer Vision and Pattern Recognition*, pp. 5710–5719, 2020.
- Cubuk, E. D., Zoph, B., Mane, D., Vasudevan, V., and Le, Q. V. Autoaugment: Learning augmentation strategies from data. In *Proceedings of the IEEE/CVF Conference on Computer Vision and Pattern Recognition*, pp. 113–123, 2019.
- Epalle, T. M., Song, Y., Liu, Z., and Lu, H. Multi-atlas classification of autism spectrum disorder with hinge loss trained deep architectures: Abide i results. *Applied Soft Computing*, 107:107375, 2021. ISSN 1568-4946. doi: <https://doi.org/10.1016/j.asoc.2021.107375>. URL <https://www.sciencedirect.com/science/article/pii/S1568494621002982>.
- Gentile, C. and Warmuth, M. K. Linear hinge loss and average margin. *Advances in neural information processing systems*, 11, 1998.
- Genz, A. Numerical computation of multivariate normal probabilities. *Journal of computational and graphical statistics*, 1(2):141–149, 1992.
- Goan, E. and Fookes, C. Bayesian neural networks: An introduction and survey. In *Case Studies in Applied Bayesian Data Science*, pp. 45–87. Springer, 2020.
- Grabocka, J., Scholz, R., and Schmidt-Thieme, L. Learning surrogate losses. *arXiv preprint arXiv:1905.10108*, 2019.
- Han, D., Kim, J., and Kim, J. Deep pyramidal residual networks. In *Proceedings of the IEEE conference on computer vision and pattern recognition*, pp. 5927–5935, 2017.
- He, K., Zhang, X., Ren, S., and Sun, J. Deep residual learning for image recognition. In *Proceedings of the IEEE conference on computer vision and pattern recognition*, pp. 770–778, 2016.
- Jin, J., Fu, K., and Zhang, C. Traffic sign recognition with hinge loss trained convolutional neural networks. *IEEE transactions on intelligent transportation systems*, 15(5): 1991–2000, 2014.
- Karpukhin, I., Dereka, S., and Kolesnikov, S. Probabilistic embeddings revisited. *arXiv preprint arXiv:2202.06768*, 2022.
- Kaya, M. and Bilge, H. Ş. Deep metric learning: A survey. *Symmetry*, 11(9):1066, 2019.
- Kingma, D. P. and Ba, J. Adam: A method for stochastic optimization. *arXiv preprint arXiv:1412.6980*, 2014.
- Kingma, D. P. and Welling, M. Auto-encoding variational bayes. In Bengio, Y. and LeCun, Y. (eds.), *2nd International Conference on Learning Representations, ICLR 2014, Banff, AB, Canada, April 14-16, 2014, Conference Track Proceedings*, 2014.
- Krizhevsky, A., Hinton, G., et al. Learning multiple layers of features from tiny images. 2009.
- Krizhevsky, A., Sutskever, I., and Hinton, G. E. Imagenet classification with deep convolutional neural networks. *Advances in neural information processing systems*, 25, 2012.
- Kwon, J., Kim, J., Park, H., and Choi, I. K. Asam: Adaptive sharpness-aware minimization for scale-invariant learning of deep neural networks. In *International Conference on Machine Learning*, pp. 5905–5914. PMLR, 2021.
- LeCun, Y., Bottou, L., Bengio, Y., and Haffner, P. Gradient-based learning applied to document recognition. *Proceedings of the IEEE*, 86(11):2278–2324, 1998.
- Maas, A., Daly, R. E., Pham, P. T., Huang, D., Ng, A. Y., and Potts, C. Learning word vectors for sentiment analysis. In *Proceedings of the 49th annual meeting of the association for computational linguistics: Human language technologies*, pp. 142–150, 2011.
- Netzer, Y., Wang, T., Coates, A., Bissacco, A., Wu, B., and Ng, A. Y. Reading digits in natural images with unsupervised feature learning. 2011.
- Ozyildirim, B. M. and Kiran, M. Levenberg–marquardt multi-classification using hinge loss function. *Neural Networks*, 143:564–571, 2021. ISSN 0893-6080. doi: <https://doi.org/10.1016/j.neunet.2021.07.010>. URL <https://www.sciencedirect.com/science/article/pii/S0893608021002732>.
- Paszke, A., Gross, S., Massa, F., Lerer, A., Bradbury, J., Chanan, G., Killeen, T., Lin, Z., Gimelshein, N., Antiga, L., et al. Pytorch: An imperative style, high-performance deep learning library. *Advances in neural information processing systems*, 32, 2019.

- Patel, Y., Toliás, G., and Matas, J. Recall@ k surrogate loss with large batches and similarity mixup. *arXiv preprint arXiv:2108.11179*, 2021.
- Peng, H. and Liu, C.-L. Discriminative feature selection via employing smooth and robust hinge loss. *IEEE Transactions on Neural Networks and Learning Systems*, 30(3): 788–802, 2018.
- Rosasco, L., De Vito, E., Caponnetto, A., Piana, M., and Verri, A. Are loss functions all the same? *Neural computation*, 16(5):1063–1076, 2004.
- Shi, Y. and Jain, A. K. Probabilistic face embeddings. In *Proceedings of the IEEE/CVF International Conference on Computer Vision*, pp. 6902–6911, 2019.
- Sutskever, I., Martens, J., Dahl, G., and Hinton, G. On the importance of initialization and momentum in deep learning. In *International conference on machine learning*, pp. 1139–1147. PMLR, 2013.
- Tan, M. and Le, Q. Efficientnet: Rethinking model scaling for convolutional neural networks. In *International conference on machine learning*, pp. 6105–6114. PMLR, 2019.
- Wang, Q., Ma, Y., Zhao, K., and Tian, Y. A comprehensive survey of loss functions in machine learning. *Annals of Data Science*, 9(2):187–212, 2022.
- Weinberger, K. Q. and Saul, L. K. Distance metric learning for large margin nearest neighbor classification. *Journal of machine learning research*, 10(2), 2009.
- Zagoruyko, S. and Komodakis, N. Wide residual networks. *arXiv preprint arXiv:1605.07146*, 2016.
- Zhang, X., Zhao, J., and LeCun, Y. Character-level convolutional networks for text classification. *Advances in neural information processing systems*, 28, 2015.

A. Proofs

Theorem 4.2. Suppose scores vector s is distributed according to multivariate normal distribution $\mathcal{N}(\mu, \sigma^2 I)$ in \mathbb{R}^C . Then probability of the y -th score exceeding other scores can be computed as

$$P(s_y > \max_{i \neq y} s_i) = \int_{\Omega_+} \mathcal{N}(t; \frac{D_y \mu}{\sigma}, D_y D_y^T) dt, \quad (19)$$

where D_y is a delta matrix of the order C for label y and $\Omega_+ : \{t \in \mathbb{R}^{C-1}, t_i \geq 0, i = \overline{1, C-1}\}$ is an orthant in \mathbb{R}^{C-1} .

Proof. Let's rewrite Equation 19:

$$P(s_y > \max_{i \neq y} s_i) = P(s_y - \max_{i \neq y} s_i > 0) \quad (20)$$

$$= P(\min_{i \neq y} (s_y - s_i) > 0). \quad (21)$$

Due to the definition of the delta matrix D_y , vector $d = D_y s$ is a $(C-1)$ -dimensional vector with elements equal to differences between score of the ground truth class y and other scores:

$$d_i = \begin{cases} s_y - s_i, & i < y \\ s_y - s_{i+1}, & i \geq y \end{cases}, \quad (22)$$

so

$$P(s_y > \max_{i \neq y} s_i) = P(\min_i d_i > 0) \quad (23)$$

$$= P(\min_i \frac{d_i}{\sigma} > 0) \quad (24)$$

$$= P(\min_i w_i > 0), \quad (25)$$

where $w = \frac{D_y s}{\sigma}$. Due to the properties of the multivariate normal distribution, random vector w is also normally distributed:

$$w \sim \mathcal{N}(\frac{D_y \mu}{\sigma}, D_y D_y^T). \quad (26)$$

Finally:

$$P(s_y > \max_{i \neq y} s_i) = P(w_1 > 0, \dots, w_{C-1} > 0) \quad (27)$$

$$= \int_{\Omega_+} \mathcal{N}(t; \frac{D_y \mu}{\sigma}, D_y D_y^T) dt. \quad (28)$$

□

Theorem 4.3. Suppose vector s is distributed according to multivariate normal distribution $\mathcal{N}(m, \Sigma)$ in \mathbb{R}^{C-1} and \hat{s}_i is a random vector of all elements in s except i -th, conditioned on $s_i = -m_i$. Then \hat{s}_i is normally-distributed with

some parameters \hat{m}_i and $\hat{\Sigma}_i$ and

$$\left(\int_{\Omega_+} \mathcal{N}(t; m, \Sigma) dt \right)'_{m_i} = \mathcal{N}(0; m_i, \Sigma_{i,i}) \int_{\Omega'_+} \mathcal{N}(t; \hat{m}_i, \hat{\Sigma}_i) dt, \quad (29)$$

where $\Omega'_+ : \{t \in \mathbb{R}^{C-2}, t_i \geq 0, i = \overline{1, C-2}\}$ is an orthant in \mathbb{R}^{C-2} .

Proof.

$$\int_{\Omega_+} \mathcal{N}(t; m, \Sigma) dt \quad (30)$$

$$= \int_0^\infty \dots \int_0^\infty \mathcal{N}(t; m, \Sigma) dt_{C-1} \dots dt_1 \quad (31)$$

$$= \int_0^\infty \dots \int_0^\infty \mathcal{N}(t - m; 0, \Sigma) dt_{C-1} \dots dt_1 \quad (32)$$

$$= \int_{-m_1}^\infty \dots \int_{-m_{C-1}}^\infty \mathcal{N}(t; 0, \Sigma) dt_{C-1} \dots dt_1 \quad (33)$$

Assume, without loss of generality, that $i = 1$. Then we can find derivative using Leibniz integral rule:

$$\left(\int_{\Omega_+} \mathcal{N}(t; m, \Sigma) dt \right)'_{m_1} \quad (34)$$

$$= \int_{-m_2}^\infty \dots \int_{-m_{C-1}}^\infty \mathcal{N}(t; 0, \Sigma) dt_{C-1} \dots dt_2 \Big|_{t_1 = -m_1} \quad (35)$$

$$= \int_0^\infty \dots \int_0^\infty \mathcal{N}(t; m, \Sigma) dt_{C-1} \dots dt_2 \Big|_{t_1 = 0} \quad (36)$$

Integration region in the last integral is a positive orthant Ω'_+ , which is a lower dimension subset of Ω_+ :

$$\left(\int_{\Omega_+} \mathcal{N}(t; m, \Sigma) dt \right)'_{m_1} = \int_{\Omega'_+} \mathcal{N}(t; m, \Sigma) dt_{C-1} \dots dt_2 \Big|_{t_1 = 0}. \quad (37)$$

We can decompose inner density using properties of the multivariate normal distribution:

$$P_s(t) = P_s(t_1, \dots, t_{C-1}) \quad (38)$$

$$= P_s(t_1, t_{2:C-1}) \quad (39)$$

$$= P_{s_1}(t_1)P_{s_{2:C-1}}(t_{2:C-1}|s_1 = t_1), \quad (40)$$

so

$$\mathcal{N}(t; m, \Sigma) = \mathcal{N}(t_1; m_1, \Sigma_{1,1})\mathcal{N}(t_{2:C-1}; \hat{m}_1, \hat{\Sigma}_1), \quad (41)$$

where \hat{m}_1 and $\hat{\Sigma}_1$ are parameters of the conditional distribution from Equation 40:

$$\hat{m}_1 = m_{2:C-1} + \Sigma_{2:C-1,1}\Sigma_{1,1}^{-1}(t_1 - m_1), \quad (42)$$

$$\hat{\Sigma}_1 = \Sigma_{2:C-1,2:C-1} - \Sigma_{2:C-1,1}\Sigma_{1,1}^{-1}\Sigma_{1,2:C-1}. \quad (43)$$

Pitting Equation 41 to Equation 37 finally proves the theorem. \square

B. Implementation Notes

A considerable boost in EXACT performance can be obtained from analysis of the matrix $\Sigma = D_y D_y^T$ in Equation 19. Matrix D_y is a delta matrix for the label y :

$$D_y = \begin{bmatrix} -1 & 0 & \dots & 0 & 1 & 0 & \dots & 0 \\ 0 & -1 & \dots & 0 & 1 & 0 & \dots & 0 \\ & & \ddots & & \vdots & & \ddots & \\ 0 & 0 & \dots & -1 & 1 & 0 & \dots & 0 \\ 0 & 0 & \dots & 0 & 1 & -1 & \dots & 0 \\ & & \ddots & & \vdots & & \ddots & \\ 0 & 0 & \dots & 0 & 1 & 0 & \dots & -1 \end{bmatrix}. \quad (44)$$

It can be seen, that $D_y D_y^T$ is independent of y :

$$\Sigma = D_y D_y^T = \begin{bmatrix} 2 & 1 & \dots & 1 \\ 1 & 2 & \dots & 1 \\ & & \ddots & \\ 1 & 1 & \dots & 2 \end{bmatrix}. \quad (45)$$

Matrix Σ and its Cholesky decomposition, used in Genz algorithm, can be computed before training. At the same time, the special form of Σ largely simplifies equations for computing \hat{m}_i and $\hat{\Sigma}_i$.

Cholesky decomposition of the matrix Σ has the following form:

$$L = \begin{bmatrix} \alpha_1 & 0 & \dots & 0 \\ \beta_1 & \alpha_2 & \dots & 0 \\ & & \ddots & \\ \beta_1 & \beta_2 & \dots & 0 \\ \beta_1 & \beta_2 & \dots & \alpha_{C-1} \end{bmatrix}. \quad (46)$$

Note, that elements in each column below diagonal are the same. Genz algorithm can be optimized to make use of this property of the matrix L .